Molecular insights of the first gastropod TLR counterpart from disk abalone (Haliotis discus discus) revealing its transcriptional modulation under pathogenic stress

Article *in* Fish & Shellfish Immunology · May 2013

DOI: 10.1016/j.fsi.2013.04.031 · Source: PubMed

CITATIONS
14

READS
87

5 authors, including:

Don Anushka Sandaruwan Elvitigala
University of Colombo
63 PUBLICATIONS **240** CITATIONS
SEE PROFILE

H.K. Ajith Premachandra
University of Peradeniya
52 PUBLICATIONS **176** CITATIONS
SEE PROFILE

Ilson Whang
150 PUBLICATIONS **2,292** CITATIONS
SEE PROFILE

Bo-Hye Nam
National Fisheries Research and Development Institution
265 PUBLICATIONS **2,125** CITATIONS
SEE PROFILE

Fish & Shellfish Immunology 35 (2013) 334–342

Contents lists available at SciVerse ScienceDirect

Fish & Shellfish Immunology

journal homepage: www.elsevier.com/locate/fsi

Molecular insights of the first gastropod TLR counterpart from disk abalone (*Haliotis discus discus*), revealing its transcriptional modulation under pathogenic stress

Don Anushka Sandaruwan Elvitigala [a], H.K.A. Premachandra [a], Ilson Whang [a,*], Bo-Hye Nam [b], Jehee Lee [a,c,*]

[a] Department of Marine Life Sciences, School of Marine Biomedical Sciences, Jeju National University, Jeju Self-Governing Province 690-756, Republic of Korea
[b] Biotechnology Research Division, National Fisheries Research and Development Institute (NFRDI), 408-1 Sirang-ri, Gijang-eup, Gijang-gun, Busan 619-705, Republic of Korea
[c] Marine and Environmental Institute, Jeju National University, Jeju Special Self-Governing Province 690-814, Republic of Korea

ARTICLE INFO

Article history:
Received 29 November 2012
Received in revised form
3 April 2013
Accepted 22 April 2013
Available online 10 May 2013

Keywords:
Novel TLR homolog
Disk abalone
Phylogenetic relationship
Spatial expression of mRNA
Transcriptional profiles under pathogenic stress

ABSTRACT

Toll-like receptors (TLRs) are well-characterized pattern recognition receptors of innate immunity, known to induce immune responses against the pathogens by interacting with evolutionarily conserved pathogen-associated molecular patterns (PAMPs). In this study, a novel TLR homolog from disk abalone (*Haliotis discus discus*) was identified and characterized at molecular level. The open reading frame (ORF) of *AbTLR* is 3804 bp in length and encodes a 1268 amino acid peptide with a calculated molecular mass of 143.5 kDa. The deduced protein shows typical TLR domain architecture, with leucine rich repeats (LRR) and the toll-interleukin receptor (TIR) domain. Phylogenetic analysis revealed a close evolutionary relationship for AbTLR to its invertebrate counterparts, with close clustering to the molluscan homologs. Quantitative real-time PCR detected ubiquitous transcription of *AbTLR* in healthy tissues, but with highest levels in hemocytes. Differential transcriptional modulation of *AbTLR* was observed in abalone hemocytes and gills upon immune challenge, whereby *Vibrio parahaemolyticus* and purified lipopolysaccharide (LPS) enhanced the transcript level prominently. In addition, the viral hemorrhagic septicemia virus induced *AbTLR* transcription in hemocytes and gills, representing the first evidence of viral-induced immune response in mollusks to date. Collectively, our findings support a putative role for AbTLR in abalone antiviral and antibacterial defense.

1. Introduction

Invertebrates depend exclusively on innate immunity to combat infectious non self-agents, such as pathogenic microorganisms, since they do not possess an adaptive immune system. Recognition of invading pathogens to mount the innate immune response is generally mediated by the host-expressed pattern recognition receptors (PRRs), which interact with evolutionarily conserved, ubiquitously expressed molecular factors that decorate pathogenic microorganisms and are known as pathogen-associated molecular patterns (PAMPs) [1,2]. The most extensively studied PRRs are the Toll-like receptors (TLRs), and many of their PAMP ligands are well-characterized, including the lipopolysaccharide (LPS) and peptidoglycan cell wall components of bacteria and the flagellin protein, as well as free nucleic acid strands from lysed bacteria and viruses [3,4]. Moreover, these collective studies have revealed that the critical regulatory role of TLRs in innate immunity has been maintained throughout evolution, from cnidarians to mammals [5]. Indeed, recent studies demonstrating the compatibility of invertebrate and vertebrate innate immune systems have implicated the TLR-mediated immune signaling pathways as a key commonality [6,7].

The various TLR family members control different immune signaling pathways by activating a wide array of down-stream signaling molecules, such as myeloid differentiation factor 88

* Corresponding authors. Marine Molecular Genetics Lab, Department of Marine Life Sciences, College of Ocean Science, Jeju National University, 66 Jejudaehakno, Ara-Dong, Jeju, 690 756, Republic of Korea. Tel.: +82 64 754 3472; fax: +82 64 756 3493.
E-mail addresses: ilsonwhang@hanmail.net (I. Whang), jehee@jejunu.ac.kr, jeheedaum@hanmail.net (J. Lee).

1050-4648/$ – see front matter © 2013 Elsevier Ltd. All rights reserved.
http://dx.doi.org/10.1016/j.fsi.2013.04.031

(MyD88), interleukin-1 (IL-1) receptor-associated kinase (IRAK), TNF receptor-associated factors (TRAFs), and nuclear factor kappa B (NF-κB) [8]. These various TLR signaling pathways culminate in the stimulation of particular genes' expression and immune-modulatory factors' activity, such as the cytokines. However, for all known TLRs the signal originates from a cellular membrane, either the plasma membrane (TLR1, 2, 4, 5, 6, and 10) or an intracellular endosome membrane (TLR 3, 7, 8, and 9) [9]. The common transmembrane localization is reflected in the characteristic protein structure of TLRs, which includes an ectodomain that protrudes outwards and is composed of ≤26 leucine rich repeat (LRR) motifs, a transmembrane domain, and an endodomain that extend inward and contains the signature Toll/IL-1 receptor (TIR) domain [10]. The TIR domain not only mediates localization of the TLR molecule to a particular membrane region but also initiates the down-stream signaling cascade [11,12].

Even though several invertebrate TLRs have been identified to date, only a few represent the molluscan species, including *Crassostrea gigas* [13] and *Chlamys farreri* (Akazara scallop) [14]. Yet, understanding the innate immune responses of marine invertebrate species is rapidly becoming important for the global food industry. Marine invertebrates, especially mollusks and arthropods, which are used as comestibles has reached to the levels of consumption, comparable to fish in many of the world's nations, with the most prominent use being in the East and Southeastern regions of Asia, including countries like China, Korea, and Japan. As a result, abalone has emerged as an economically important delicacy of the commercial invertebrate aquaculture industry. However, these marine gastropods are sensitive to a wide range of environmental conditions, some of which cause grievous impact on survival and growth. Pathogenic infections, in particular, have emerged as prominent threats to abalone integrity as a human food source [15–17]. The fact that the natural innate immune mechanisms functioning in abalones can tolerate some of these pathological invasions, to a certain extent, suggests that these mechanisms may represent targets of disease management strategies to help sustainable commercial farming efforts.

In this study, a novel TLR homolog (AbTLR) from disk abalone (*Haliotis discus discus*) was characterized at the molecular level. Moreover, transcriptional modulation of *AbTLR* was analyzed under pathological conditions, stimulated by live bacteria and virus, as well as purified LPS, to determine its potential role in immune defense of disk abalone.

2. Materials and methods

2.1. Identification of the partial cDNA sequences of AbTLR

A disk abalone sequence database was established based upon sequencing data (Roche 454 genome sequencer FLX systems (GS-FLX™); DNA Link, Republic of Korea) of a cDNA library generated from mRNA isolated from whole tissues of disk abalone [18]. Searching of this database with the Basic Local Alignment Tool (BLAST) algorithm (http://www.ncbi.nlm.nih.gov/BLAST) led to the identification of a TLR partial length cDNA sequences (isotig18424, isotig19106 and GSPZ16V01BZ56Q).

2.2. Identification of AbTLR complete coding sequence

A random shear bacterial artificial chromosome (BAC) library of abalone genomic DNA was custom constructed (Lucigen, USA) and screened for the full-length *AbTLR* gene by using the previously described pooling and super pooling strategies followed by polymerase chain reaction (PCR) [19]. The target gene sequence-specific primer pair, AbTLR-F and AbTLR-R (Table 1), was designed based on the partial cDNA sequence of *AbTLR* (Section 2.1). The PCR amplification was carried out in a total volume of 20 μL containing 0.5 U of Ex*Taq* polymerase (TaKaRa, Japan), 2 μL of 10× Ex*Taq* buffer, 1.6 μL of 2.5 mM dNTPs, 75 ng of template, and 10 pmol of each primer. The thermal cycling reaction included an initial 3 min incubation at 94 °C, followed by 35 cycles of 94 °C for 30 s, 58 °C for 30 s, and 72 °C for 30 s. The PCR products were analyzed on a 1.5% agarose gel and the band representing the amplicon containing the *AbTLR* gene was identified by expected size. Subsequently, detected BAC clone was sequenced (GS-FLX™) to obtain the genomic DNA sequence of the *AbTLR* gene. The complete putative coding sequence of *AbTLR* was then anticipated by analyzing the obtained genomic DNA sequence using the BLASTx algorithm and aligning with the existed partial cDNA sequences using DNAssist 2.2 (version 3.0) software. Coding sequence was further confirmed by cloning the respective fragment into pGEM-T vector (Promega – USA), after PCR amplification, using disk abalone multi tissue cDNA. Finally, the nucleotide sequence of *AbTLR* was deposited in GenBank under the accession number JX827423.

Table 1
Primers used in this study.

Name	Purpose	Sequence (5′ → 3′)
AbTLR-F	BAC library screening and qRT PCR of AbTLR	ACAGCTTCTTGGACGACGAATGGT
AbTLR-R	BAC library screening and qRT PCR of AbTLR	TCGTGCATGACGATGACGATGAGT
Ab-Rp-F	qRT-PCR of abalone ribosomal protein L5 gene	TCACCAACAAGGACATCATTTGTC
Ab-Rp-R	qRT-PCR of abalone ribosomal protein L5 gene	CAGGAGGAGTCCAGTGCAGTATG

2.3. In-silico analysis of AbTLR sequences

The nucleotide and predicted amino acid (aa) sequences of *AbTLR* were compared with those of various TLRs from different species that were retrieved by the BLAST search program. Pairwise sequence alignment and multiple sequence alignment were performed using the ClustalW2 program [20]. The phylogenetic relationship of these homologs was assessed by the Molecular Evolutionary Genetics Analysis (MEGA) software (version 5) using the neighbor-joining method with bootstrap values taken from 1000 replicates [21]. The characteristic TLR protein signatures were predicted by the ExPASy-Prosite server (http://prosite.expasy.org) and the SMART online server (http://smart.embl-heidelberg.de). The ExPASy protParam tool (http://web.expasy.org/protparam) was used to predict some physicochemical properties of the AbTLR protein. Furthermore, in order to prefigure and compare the three dimensional arrangement of the TLR primary protein structure, attributing to its committed role in physiology, degree of folding throughout the whole sequence area of AbTLR as well as its two homologues molluscan counterparts from *C. farreri* and *C. gigas* were predicted using FoldIndex© online bioinformatic tool [22]. Domain architectures of all three TLRs were identified using SMART online server.

2.4. Experimental animals and tissue collection

Healthy disk abalones (*H. discus discus*), with an average weight of 50 g and size of 8 cm, were purchased from the Youngsoo Abalone Farm of Jeju Island (Republic of Korea). Upon arrival, the live abalones were acclimated to the laboratory environment (seawater tanks with continuous filtering and aeration; salinity:

33 ± 1 psu; temperature: 20 ± 1 °C) for one week prior to any experimentation. Abalones were fed daily with fresh marine seaweed (*Undaria pinnatifida*). Hemolymph was collected from pericardial cavities of three healthy, unchallenged animals, using sterilized syringes; samples were immediately centrifuged (3000 × *g* at 4 °C for 10 min) to harvest the hemocytes. Tissues from adductor muscle, mantle, gill, hepatopancreas, digestive tract and gonads were collected from three animals, snap-frozen in liquid nitrogen, and stored at −80 °C.

2.5. Immune challenge experiment

For intact Gram-negative bacterial challenge, 100 μL of *Vibrio parahemolyticus* (1×10^4 cell/mL in saline) was intramuscularly injected into healthy, acclimated abalones. For virus challenge, a Korean isolate of viral hemorrhagic septicemia virus (VHSV; FWando05 from an infected olive flounder (*Paralichthys olivaceus*)) was first amplified by inoculation of cultured fathead minnow (FHW) cells and growth in Dulbecco's modified Eagle's minimum essential medium (DMEM) supplemented with antibiotics and 10% fetal bovine serum (FBS). When the cytopathic effect was extensive, the virus-containing supernatant was harvested and centrifuged to eliminate cell debris. Healthy, acclimated abalones were administered a single intramuscular injection of 100 μL of VHSV (1×10^8 pfu/mL in saline). For the purified endotoxin challenge, abalones were injected intramuscularly with 100 μL of LPS (500 μg/animal, which equaled a dose of ~10 mg/kg; *Escherichia coli* 0127:B8 from Sigma, USA). Control groups were established for each immune challenge experiment and included un-injected healthy, acclimated abalones (negative controls) and saline-injected healthy, acclimated abalones (equal volume to the challenge injection; positive controls). At 3, 6, 12, 24, 48 and 72 h post-injection (p.i.), gill tissues were collected and hemolymph was extracted for hemocyte harvesting (Section 2.4) from at least four abalones of control and challenged groups for subsequent quantitative real time PCR (qRT-PCR) analysis.

2.6. Total RNA extraction and cDNA synthesis

Total RNA was extracted from tissues of at least four abalones by the Tri-Reagent™ (Sigma). After spectrophotometric quantification (optical density at 260 nm; Bio-Rad, USA), the purified total RNA samples were diluted to 1 μg/μL and pooled to perform multi-tissue cDNA synthesis (PrimeScript™ cDNA Synthesis Kit; TaKaRa, Japan). Finally, the newly-synthesized cDNA was diluted 40-fold (800 μL total volume) and stored at −20 °C.

2.7. AbTLR mRNA expression analysis by qRT-PCR

qRT-PCR was used to detect the normal tissue distribution of *AbTLR* expression, as well as the immune-responsive and temporal expression in hemocytes and gills. The qRT-PCR was carried out in 15 μL reaction volumes composed of 4 μL of diluted cDNA from the respective tissue, 7.5 μL of 2× TaKaRa Ex*Taq* SYBR Green premix, 0.6 μL of each primer (AbTLR-F and AbTLR-R), and 2.3 μL of double-deionized (dd) H_2O. A Dice™ Real Time System (TP800; TaKaRa) was used with the following thermal cycling conditions: 95 °C for 10 s, followed by 35 cycles of 95 °C for 5 s, 58 °C for 10 s and 72 °C for 20 s, and a final cycle of 95 °C for 15 s, 60 °C for 30 s and 95 °C for 15 s. The same qRT-PCR cycle profile was used for measuring expression of the internal control gene, abalone ribosomal protein L5 (GenBank Accession No. EF103443), with the respective gene-specific primers (Table 1). For all reactions, the Dice™ Real Time System Software (version 2.00) automatically determined the baseline fluorescence. The amount of *AbTLR* expression was determined by the Livak ($2^{-\Delta\Delta CT}$) method [23]. Each sample was analyzed in triplicate and the data calculated as mean ± standard deviation (SD) of relative mRNA expression. To determine the statistical significance ($P < 0.05$) of expression differences between an experimental group and the negative control group (un-injected animals), a two-tailed paired *t*-test was carried out.

3. Results and discussion

3.1. Sequence characterization

The complete coding region of *AbTLR* was comprised of 3804 bps, encodes for a peptide of 1268 aa. The encoded AbTLR had a predicted molecular mass of ~143.5 kDa and theoretical isoelectric point of ~6.1.

The overall protein sequence of AbTLR resembled the typical TLR domain architecture, including an ectodomain with the maximum number of LRR motifs (26) and N- and C-terminal LRR modules, a transmembrane domain, and an endodomain with a TIR motif (Figs. 1 and 2). The SMART online server identified an initial signal peptide of 21 aa (Figs. 1 and 2), which agrees with the cell surface localization of many TLRs. The fact that the AbTLR contains a maximum number of LRRs may indicate a broad-range capacity for recognition of different PAMPs; indeed, an increased number of LRR motifs increases the surface area of the ectodomain and its ability to interact with a broader spectrum of ligands of different infectious microorganisms [24]. When the domain architecture of AbTLR was compared with that of other invertebrate TLRs (Fig. 2), the molluscan TLRs showed a similar signal peptide, suggesting a similar character on the extracellular component of the transmembrane protein. Although the other TLRs from insects lack signal peptides, they contain the maximum number of LRRs in their ectodomain; thus, the ectodomain of AbTLR has higher similarity to insect TLRs than to molluscan TLRs (Fig. 2).

As depicted in Fig. 3, showing a compatibility with *C. farreri and C. gigas* counterparts, AbTLR was predicted to be almost well structured throughout the whole protein sequence due to folded structure. Particularly, transmembrane regions were detected to be prominently structured, depicting a highest level of folding. According to a previous report, transmembrane domains of some TLRs can actively participate in oligomerization with other TLRs, rendering heterotopic interactions [25]. In general, folded protein structures can easily exert this type of interactions rather than disordered ones. Therefore, highly structured arrangements of the transmembrane domains of the TLRs used in our prediction might attribute to their potential interactions with other TLR members to form oligomers. Substantial level of folding of N − termini, which covers the ectodomain can obviously be attributed to the significant amount of LRRs identified in that region (Fig. 2). However, as a common feature of all three TLRs, end of the C terminal regions was found to be disordered compared to the N-terminal region, which does not contain any functionally important signatures, as per the *in-silico* predictions. With respect to AbTLR and its counterpart from *C. farreri*, the degree as well as the portion of disordering in unstructured regions which aligned with TIR were appeared to be negligible compared to the folded portions, convincing the positive correlation between protein folding and protein–protein interactions, since TIR is known to be the initiator of TLR signaling cascades through its interaction with the respective adaptor proteins [26]. Nevertheless, not only the order of disordering at the beginning of the TIR in *C. gigas* TLR (residues:1111-1115) was observed to be significant compared to the degree of folding in structured region, but also the region covers the TIR exhibited relatively less foldindex

compared to those in other two counterparts. This observation may be a reflection of lesser efficacy attributed with *C. gigas* TIR in signal transduction.

3.2. Sequence comparison

The pairwise sequence alignment performed by the ClustalW2 program revealed that the complete AbTLR protein sequence shares varying extents of low identity and similarity with the TLRs of other species, but the conservation of the TIR domains is substantial (Table 2). Considering the overall sequence of AbTLR, the highest percentage similarity (51.0%) and identity (31.5%) was found with the TLR from *C. farreri*. However, when the AbTLR TIR domain was considered alone, the greatest identity (60.1%) was found with the TIR from *Aedes aegypti* and the highest similarity (80.4%) was found with the TIR domain of *C. farreri*.

According to the multiple sequence alignment, most of the leucine residues in the LRR motifs of AbTLR were well-conserved among the other invertebrate TLRs (Fig. 2). Furthermore, the consensus aa sequences of the various TLRs were generally found in the TIR domains and included the FW motif of TIR [26], which plays an important role in cellular localization of TLRs. The presence of these TLR characteristic aa structural features substantiate the notion of AbTLR as a novel TLR homolog.

3.3. Phylogenetic analysis

In order to analyze the evolutionary relationship of AbTLR with other invertebrate and vertebrate similitudes, a phylogenetic tree was generated. As expected, the vertebrate and invertebrate TLRs formed two distinct clusters (Fig. 4). However, fruit fly (*Drosophila melanogaster*) was found to bear three paralogs of toll-9 which were clustered separately in a sub group under the main vertebrate cluster, close to the mammalian clade of TLR 6, showing a clear deviation from invertebrates homologues and closer evolutionary relationship with mammalian counterparts, as detected with some of the members of fruit fly toll family [27]. The AbTLR was located in the molluscan clade in the invertebrate cluster and was close to the *C. farreri* TLR sub-group (Fig. 4). This evolutionary relationship indicates a common invertebrate ancestral origin for *AbTLR*, and further suggests potential commonalities with the molluscan TLRs.

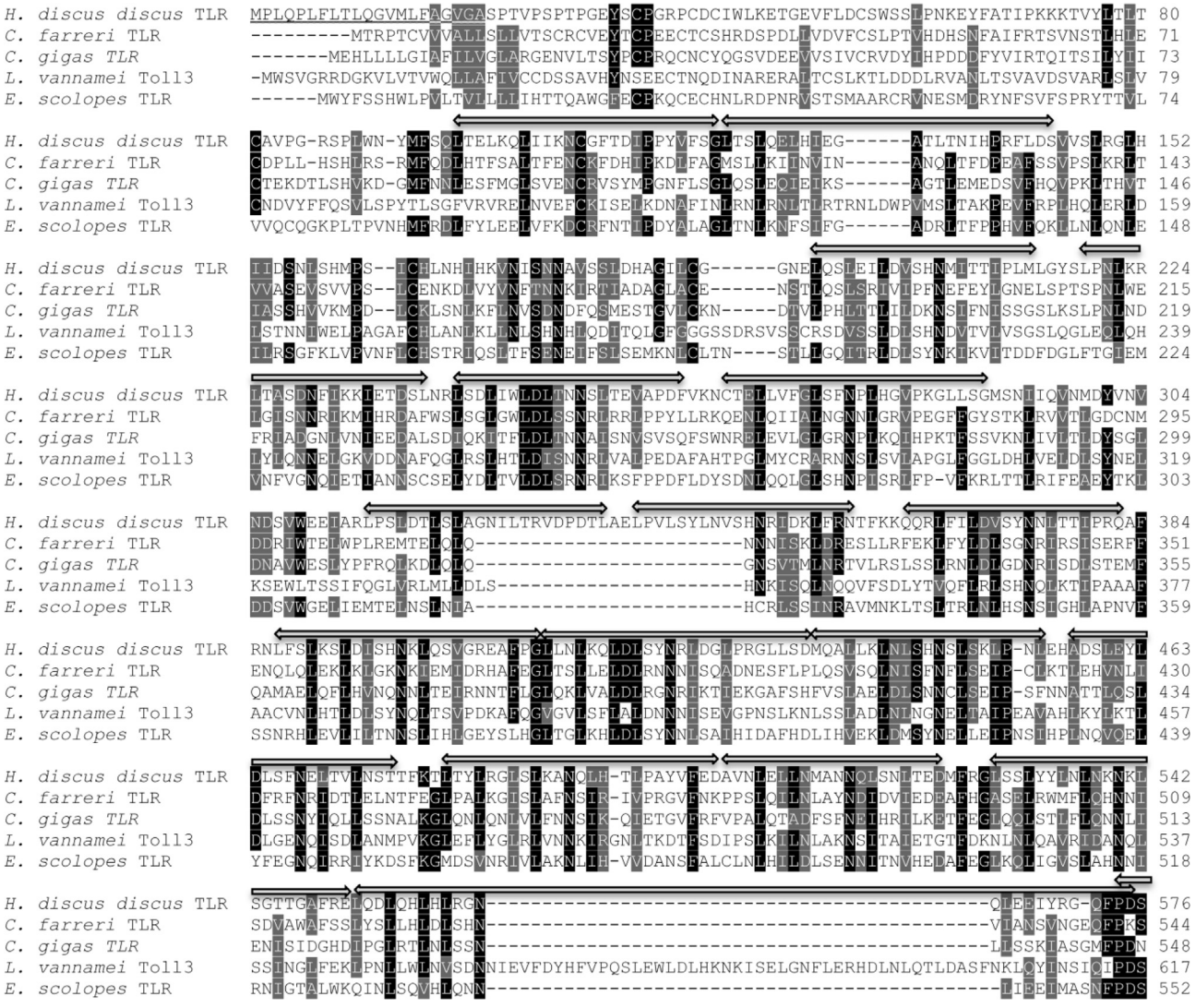

Fig. 1. Multiple sequence alignment of invertebrate TLRs. Identical and similar amino acids among the sequences are shaded in black and gray, respectively. The AbTLR signal peptide is indicated by a underline. LRR motifs are indicated by gray double-headed arrows; the C-terminal LRR is indicated by a solid black double-headed arrow and the N-terminal LRR is indicated by a pattern-filled double-headed arrow. The transmembrane domain is indicated by a thick black solid-bordered double-headed arrow. The TIR domain is indicated by a thick black discontinuous-border double-headed arrow, and the domain's conserved consensus amino acid sequences are boxed.

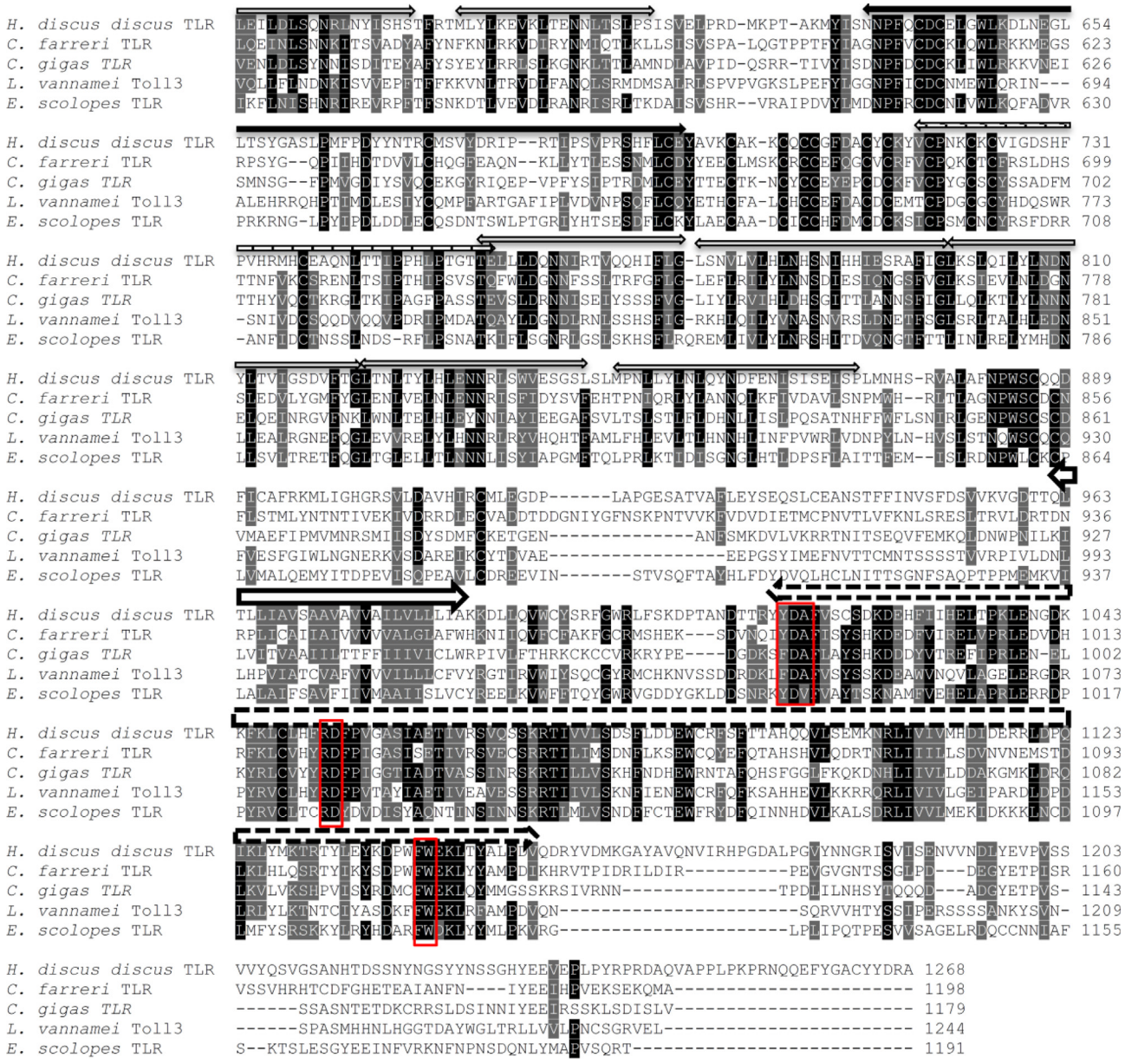

Fig. 1. (*continued*).

It is also intriguing to note that, unlike the vertebrate TLRs and the non-molluscan invertebrate TLRs, all of the molluscan TLRs used in the study, including AbTLR, which were separately clustered in the invertebrate clade cannot be categorized under any known TLR subfamily, affirming their structural and functional novelty, compared to known counterparts of other invertebrates and vertebrates.

3.4. Tissue-specific expression profile of AbTLR

In order to speculate on the potential physiological role of AbTLR, its mRNA expression profile was determined by investigating the major tissues, including immune-related tissues of healthy abalones (Fig. 5). *AbTLR* was found to be expressed ubiquitously in every tissue examined; however, comparison of the relative expression levels detected in each tissue indicated that the highest transcript level occurred in hemocytes and the lowest occurred in gill tissue. Although the relative expression levels in muscle, testis (male gonad), mantle, hepatopancreas, and digestive tract were lower than that in hemocytes, they were remarkably higher than that in gill tissue. Interestingly, the previously identified tissue-specific expression profiles of TLRs from the two molluscan species, *C. gigas* [13] and *C. farreri* [14], also showed that the strongest expression occurred in hemocytes. Furthermore, the lowest level of TLR expression in *C. farreri* was also detected in the gill tissue, while the lowest levels of TLR expression in *C. gigas* were detected in the gonad and digestive gland. Hemocytes are potent immune cells that mediate infection clearance by phagocytosis or encapsulating invading pathogens [28]. Hemocytes also secrete humoral immunity factors, such as lysozyme enzymes, aminopeptidases, lectins and antimicrobial molecules, all of which are directly involved in elimination of pathogenic organisms [29,30]. We speculate that the abundant transcript level of *AbTLR* in hemocytes is likely correlated with the overall immune defense role of hemocytes.

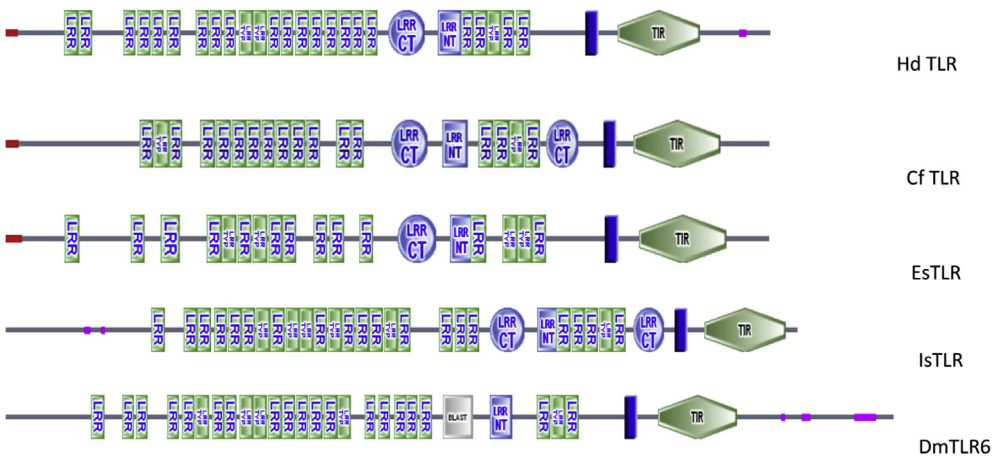

Fig. 2. Schematic structures of TLR from invertebrate homologs from *Haliotis discus discus* (Hd), *Chlamys farreri* (Cf), *Euprymna scolopes* (Es), *Ixodes scapularis* (Is), and *Drosophila melanogaster* (Dm), derived using SMART online server. The signal peptides are depicted as small, red horizontal boxes. The LRR motifs are depicted as light green vertical boxes. The C-terminal LRRs ("LRR-CT") are depicted as blue ovals, and the N-terminal LRRs ("LRR-NT") are depicted as blue boxes. The transmembrane domains are depicted as solid blue vertical boxes. Purple boxes represent the segments of low compositional complexity determined by the SEG program [38] and gray color 'BLAST' boxes indicate the hits only detected by NCBI-BLAST search. (For interpretation of the references to color in this figure legend, the reader is referred to the web version of this article.)

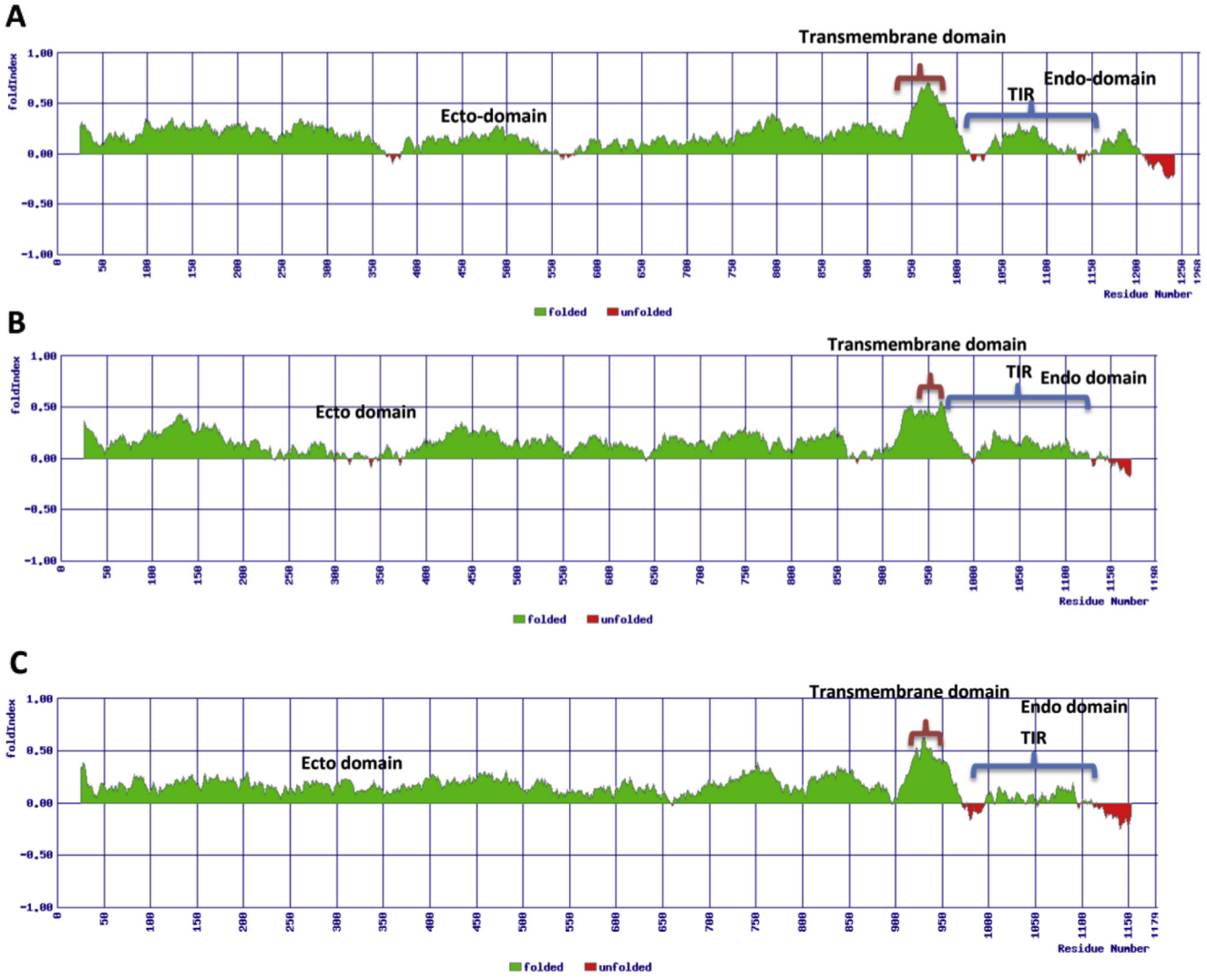

Fig. 3. Folding predictions of AbTLR (A) and its counterparts from *C. farreri* (B) and *C. gigas* (C) using FoldIndex© program. Green color areas represent the folded state whereas red color shaded regions were predicted to be unfold. Corresponding domain architectures were denoted within the respective range amino acids with their particular signatures, as predicted by SMART online server. (For interpretation of the references to color in this figure legend, the reader is referred to the web version of this article.)

Table 2
Percentage similarity and identity of AbTLR gene and its TIR domain with invertebrate TLR homologs and their respective TIR domains.

Species (common name): TLR type	Entire sequence			TIR domain		
	Identity, %	Similarity, %	Length, aa	Identity, %	Similarity, %	Length, aa
Aedes aegypti (Mosquito): TLR	28.2	43.3	1343	60.1	79.7	138
Chlamys farreri (Akazara scallop): Toll receptor	31.5	51.0	1198	56.5	80.4	138
Litopenaeus vannamei (Shrimp): TLR3	27.1	45.0	1244	54.3	76.1	138
Ixodes scapularis (Blacklegged tick): TLR	26.3	39.9	1344	46.0	68.3	138
Euprymna scolopes (Squid): TLR	26.2	44.8	1191	39.1	63.0	138
Crassostrea gigas (Pacific oyster): TLR	29.8	47.5	1169	37.0	63.8	137
Drosophila melanogaster (Fruit fly): TLR6	23.7	37.4	1514	36.2	63.0	136
Drosophila melanogaster (Fruit fly): TLR7	23.6	39.9	1446	27.0	46.1	133

3.5. Transcriptional responses of AbTLR upon immune induction

In order to evaluate the potential role of AbTLR in abalone immunity, the transcriptional responsiveness of *AbTLR* upon exposure to the *V. parahemolyticus* bacterial pathogen, the VHSV viral pathogen, and the LPS PAMP was temporally analyzed in hemocytes and gill by qRT-PCR. In most of the marine molluscan species, the gills function as the basic respiratory organ; the gills' continuous exposure to the external environment is accompanied by a continuous barrage of potential invading pathogens and immune-stimulants [31]. Accordingly, abalone gill tissue and hemocytes were selected to analyze the immune-responsiveness of *AbTLR*, even though the *AbTLR* expression level in gill was relatively low under normal physiological conditions.

Upon immune stimulation with *V. parahemolyticus*, the *AbTLR* transcript level in hemocytes was significantly up-regulated at 6 h and 12 h p.i., showing around two-fold expression induction compared to the un-injected control (both $P < 0.05$; Fig. 6(A)). However, at 24 h p.i. the *AbTLR* mRNA expression level had returned to the basal level, which was maintained thereafter. In contrast, *AbTLR* transcript level in gill tissue was up-regulated at the later time points of the challenge experiment, with significant elevations being detected at 24 h and 48 h p.i. ($P < 0.05$; Fig. 6(A)). This phase difference in transcriptional modulation can be attributed to the major role, which is played by hemocytes in mollusk innate immune system, as described in section 3.4, compared to the cells in gill tissue. Similarly, LPS stimulation led to significantly up-regulated *AbTLR* expression in hemocytes at 6 h p.i. (>2-fold induction, $P < 0.05$) that then returned to the basal level at 12 h p.i. (Fig. 6(B)). Interestingly, the LPS stimulation led to significant transcriptional up-regulation at 6 h, 24 h and 48 h p.i. in gill tissue, which had reached nearly 7-fold induction at 48 h p.i. (Fig. 6(B)). The compatible transcriptional inductions noticed upon both of the above stimulations suggest that LPS may act as one of the PAMPs of

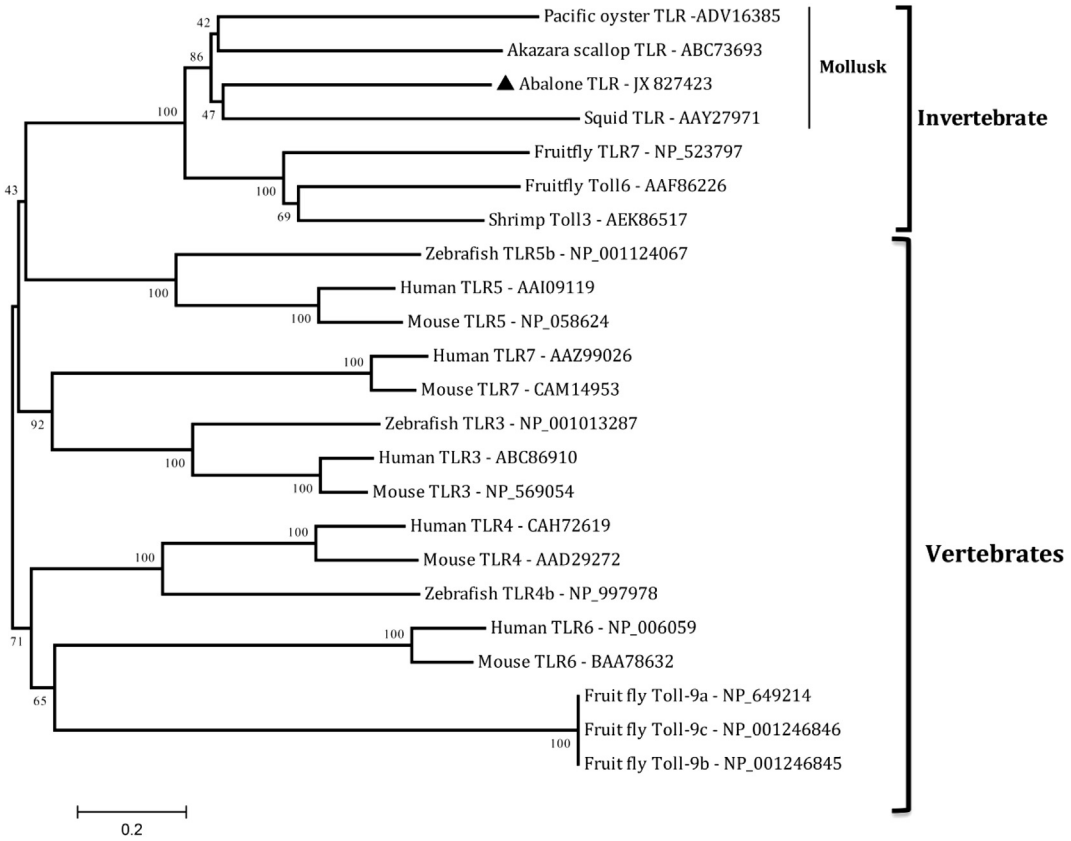

Fig. 4. Phylogenetic tree of TLR homologs. Bootstrap values are shown for each of the linages, and accession numbers of relevant TLR homologs are listed.

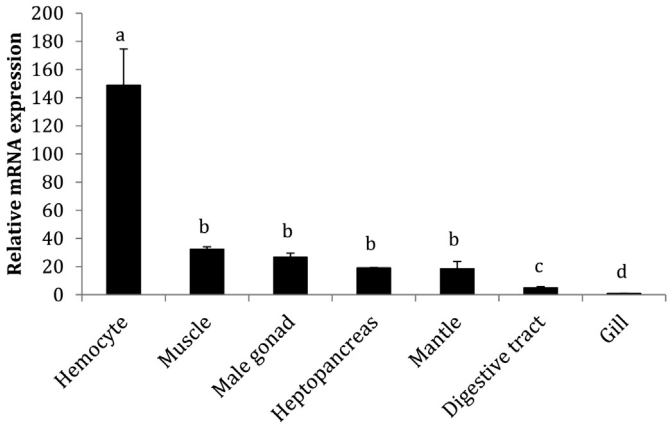

Fig. 5. Tissue-specific expression of *AbTLR*. Expression fold-changes of mRNA expression detected by qRT-PCR are presented as relative to that in gill tissue. Error bars represent the SD ($n = 3$). Expression level in every tissue was significantly different ($P < 0.05$) from the other tissues.

V. parahemolyticus that can be recognized by AbTLR, since LPS is a major cell wall component of Gram-negative bacteria [32] like *V. parahemolyticus*. Surprisingly, and in contrast to the late phase expressional profile of *AbTLR* upon bacterial stimulation, the transcript level of *AbTLR* was significantly down-regulated at 24 h and 48 h p.i. in hemocytes and at 72 h p.i. in gills (all $P < 0.05$). A previous study showed that TLR4 expression is transiently suppressed upon LPS exposure in a murine macrophage cell line, reinforcing the common observation of endotoxin tolerance in mammals [33,34]. Likewise, the *AbTLR* suppression observed at the late phase in our LPS-challenged animals might also be related to a mechanism of potential tolerance to LPS in disk abalones, possibly involving a threshold amount of TLRs expressed upon the LPS recognition that occurred at the early phase of the induction. However, further research should be carried out to confirm the exact behavior of AbTLR upon recognition of LPS, as well as to elucidate the immunological role related to this recognition process. Furthermore, early inductive response of *AbTLR* in gill tissue was triggered by LPS, compared to the live pathogen *V. parahemolyticus*, which is known to be an Gram negative bacteria bearing LPS, suggesting the rapid and less hindered interactions of PAMPs as mitogens compared to the whole pathogen due to the reduction of effective size (Fig. 6(A) and (B)). On the other hand, since *V. parahemolyticus* is a live Gram negative bacterial pathogen, TLRs can recognize multiple PAMPs apart from LPS, triggering wide array of signaling pathways and immune mechanisms [35]. Therefore, modulation pattern of AbTLR transcription can be obviously vary upon two challenges; LPS and *V. parahemolyticus*, as experienced in our experiments. Finally, it is intriguing to consider that the inductive response of *AbTLR* in hemocytes and gills upon *V. parahemolyticus* exposure agreed with the transcriptionally up-regulated expressional profile of CgToll-1 in *C. gigas* hemolymph under *Vibrio anguillarum* stress, where expression was robustly elevated at 6 h and 12 h p.i. compared to the continuously up-regulated transcript levels throughout the entire profile [13].

The VHSV challenge experiment in our disk abalones represents the first evidence of a virus-induced transcriptional response of a TLR in a molluscan species (Fig. 6(C)). Compared to the uninjected controls, the VHSV-challenged abalones showed significantly increased *AbTLR* transcript level in hemocytes distinctly at 3 h p.i. ($\sim$1.5-fold change, $P < 0.05$). However, in gill, the *AbTLR* was significantly elevated at 6 h, 48 h and 72 h p.i., with the peak fold-difference (2.5-fold) detected at 48 h p.i. (Fig. 6(C)). These inductive responses upon VHSV stimulation

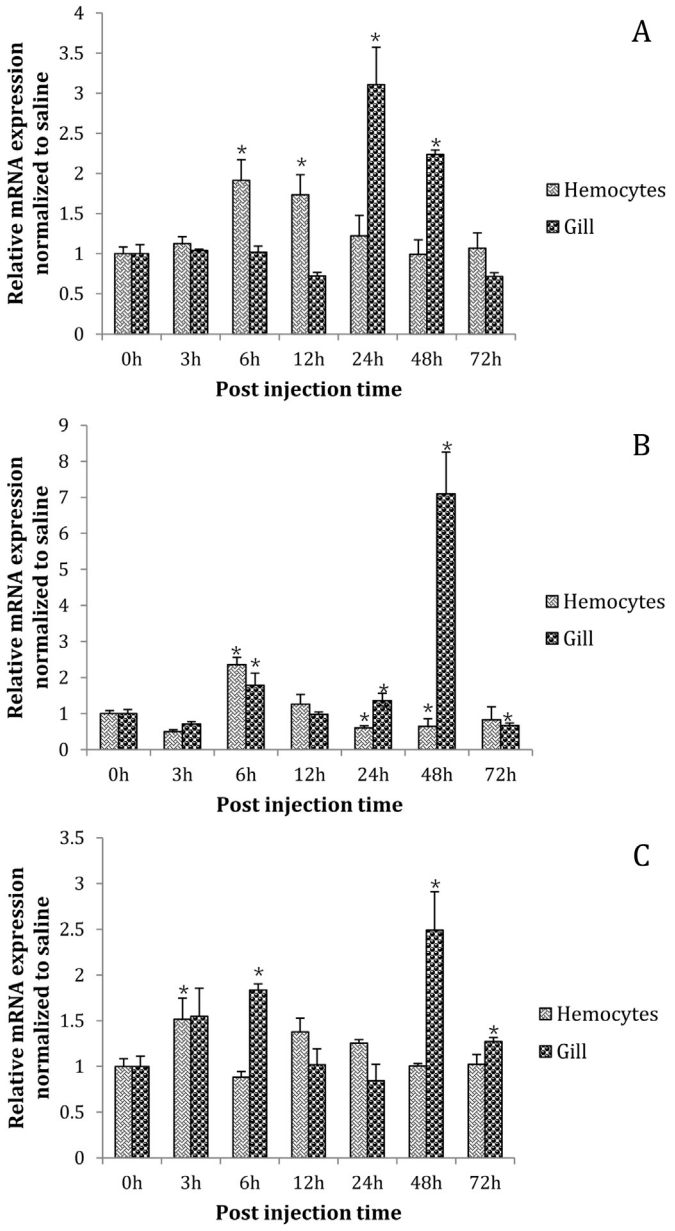

Fig. 6. Expression profile of *AbTLR* mRNA in hemocytes and gill tissues upon stimulation with (A) *V. parahaemolyticus* bacteria, (B) LPS, and (C) VHSV. The relative mRNA expression detected by qRT-PCR was calculated by the $2^{-\Delta\Delta CT}$ method, using disk abalone ribosomal protein L5 as the reference gene, and normalized to the corresponding saline-injected controls at each time point. The relevant expression fold-change at 0 h post-injection (un-injected control) was set as the baseline for comparison. Error bars represent the SD ($n = 3$); $^{*}p < 0.05$.

suggest that *AbTLR* may play a role in host immunity against viral infections through the interactions exert with the viral PAMPs like glycoproteins to activate immune signaling cascades; indeed, such a role complies with the previously reported involvement of invertebrate TLRs in host antiviral immunity, as shown in insects, such as *A. aegypti* [36], and crustaceans, such as *Litopenaeus vannamei* [37].

Altogether, these overall insights into the transcriptional modulation of *AbTLR* under pathological conditions, along with the defined protein structural signature, suggest that AbTLR may play a role in disk abalone antibacterial and antiviral defense through recognition of PAMPs, similar to the multitude of TLRs previously characterized in other vertebrate and invertebrate species.

Acknowledgment

This work was supported by a grant from the National Fisheries Research and Development Institute (RP-2013-BT-027), Republic of Korea.

References

[1] Janeway Jr CA, Medzhitov R. Innate immune recognition. Annual Review of Immunology 2002;20:197–216.
[2] Medzhitov R, Janeway Jr CA. Decoding the patterns of self and nonself by the innate immune system. Science 2002;296:298–300.
[3] Medzhitov R, Janeway Jr C. Innate immune recognition: mechanisms and pathways. Immunological Reviews 2000;173:89–97.
[4] Werling D, Jungi TW. TOLL-like receptors linking innate and adaptive immune response. Veterinary Immunology and Immunopathology 2003;91:1–12.
[5] Zheng L, Zhang L, Lin H, McIntosh MT, Malacrida AR. Toll-like receptors in invertebrate innate immunity. ISJ 2005;2:105–13.
[6] Hemmrich G, Miller DJ, Bosch TC. The evolution of immunity: a low-life perspective. Trends in Immunology 2007;28:449–54.
[7] Akira S, Takeda K, Kaisho T. Toll-like receptors: critical proteins linking innate and acquired immunity. Nature Immunology 2001;2:675–80.
[8] Martin MU, Wesche H. Summary and comparison of the signaling mechanisms of the Toll/interleukin-1 receptor family. Biochimica et biophysica acta 2002;1592:265–80.
[9] Hansen JD, Vojtech LN, Laing KJ. Sensing disease and danger: a survey of vertebrate PRRs and their origins. Developmental and Comparative Immunology 2011;35:886–97.
[10] Palti Y. Toll-like receptors in bony fish: from genomics to function. Developmental and Comparative Immunology 2011;35:1263–72.
[11] Medzhitov R. Recognition of microorganisms and activation of the immune response. Nature 2007;449:819–26.
[12] Wesche H, Henzel WJ, Shillinglaw W, Li S, Cao Z. MyD88: an adapter that recruits IRAK to the IL-1 receptor complex. Immunity 1997;7:837–47.
[13] Zhang L, Li L, Zhang G. A Crassostrea gigas Toll-like receptor and comparative analysis of TLR pathway in invertebrates. Fish & Shellfish Immunology 2011;30:653–60.
[14] Qiu L, Song L, Xu W, Ni D, Yu Y. Molecular cloning and expression of a Toll receptor gene homologue from Zhikong Scallop, Chlamys farreri. Fish & Shellfish Immunology 2007;22:451–66.
[15] Huang CY, Liu PC, Lee KK. Withering syndrome of the small abalone, Haliotis diversicolor supertexta, is caused by Vibrio parahaemolyticus and associated with thermal induction. Zeitschrift fur Naturforschung C, Journal of Biosciences 2001;56:898–901.
[16] Liu PC, Chen YC, Huang CY, Lee KK. Virulence of Vibrio parahaemolyticus isolated from cultured small abalone, Haliotis diversicolor supertexta, with withering syndrome. Letters in Applied Microbiology 2000;31:433–7.
[17] Nakatsugawa T, Nagai T, Hiya K, Nishizawa T, Muroga K. A virus isolated from juvenile Japanese black abalone Nordotis discus discus affected with amyotrophia. Disease of Aquatic Organisms 1999;36:159–61.
[18] Lee Y, De Zoysa M, Whang I, Lee S, Kim Y, Oh C, et al. Molluscan death effector domain (DED)-containing caspase-8 gene from disk abalone (Haliotis discus discus): molecular characterization and expression analysis. Fish & Shellfish Immunology 2011;30:480–7.
[19] Quiniou SM, Katagiri T, Miller NW, Wilson M, Wolters WR, Waldbieser GC. Construction and characterization of a BAC library from a gynogenetic channel catfish Ictalurus punctatus. Genetics, Selection, Evolution: GSE 2003;35:673–83.
[20] Thompson JD, Higgins DG, Gibson TJ. CLUSTAL W: improving the sensitivity of progressive multiple sequence alignment through sequence weighting, position-specific gap penalties and weight matrix choice. Nucleic Acids Research 1994;22:4673–80.
[21] Tamura K, Peterson D, Peterson N, Stecher G, Nei M, Kumar S. MEGA5: molecular evolutionary genetics analysis using maximum likelihood, evolutionary distance, and maximum parsimony methods. Molecular Biology and Evolution 2011;28:2731–9.
[22] Prilusky J, Felder CE, Zeev-Ben-Mordehai T, Rydberg EH, Man O, Beckmann JS, et al. FoldIndex: a simple tool to predict whether a given protein sequence is intrinsically unfolded. Bioinformatics 2005;21:3435–8.
[23] Livak KJ, Schmittgen TD. Analysis of relative gene expression data using real-time quantitative PCR and the 2(-Delta Delta C(T)) Method. Methods 2001;25:402–8.
[24] Bell JK, Mullen GE, Leifer CA, Mazzoni A, Davies DR, Segal DM. Leucine-rich repeats and pathogen recognition in Toll-like receptors. Trends in Immunology 2003;24:528–33.
[25] Godfroy 3rd JI, Roostan M, Moroz YS, Korendovych IV, Yin H. Isolated Toll-like receptor transmembrane domains are capable of oligomerization. PloS One 2012;7:e48875.
[26] Couture LA, Piao W, Ru LW, Vogel SN, Toshchakov VY. Targeting Toll-like receptor (TLR) signaling by Toll/interleukin-1 receptor (TIR) domain-containing adapter protein/MyD88 adapter-like (TIRAP/Mal)-derived decoy peptides. The Journal of Biological Chemistry 2012;287:24641–8.
[27] Rock FL, Hardiman G, Timans JC, Kastelein RA, Bazan JF. A family of human receptors structurally related to Drosophila Toll. Proceedings of the National Academy of Sciences of the United States of America 1998;95:588–93.
[28] Matozzo V, Rova G, Marin MG. Haemocytes of the cockle Cerastoderma glaucum: morphological characterisation and involvement in immune responses. Fish & Shellfish Immunology 2007;23:732–46.
[29] Wootton EC, Dyrynda EA, Ratcliffe NA. Bivalve immunity: comparisons between the marine mussel (Mytilus edulis), the edible cockle (Cerastoderma edule) and the razor-shell (Ensis siliqua). Fish & Shellfish Immunology 2003;15:195–210.
[30] Aton E, Renault T, Gagnaire B, Thomas-Guyon H, Cognard C, Imbert N. A flow cytometric approach to study intracellular-free Ca2+ in Crassostrea gigas haemocytes. Fish & Shellfish Immunology 2006;20:493–502.
[31] Chakraborty S, Ray M, Ray S. Toxicity of sodium arsenite in the gill of an economically important mollusc of India. Fish & Shellfish Immunology 2010;29:136–48.
[32] Raetz CR, Whitfield C. Lipopolysaccharide endotoxins. Annual Review of Biochemistry 2002;71:635–700.
[33] Poltorak A, He X, Smirnova I, Liu MY, Van Huffel C, Du X, et al. Defective LPS signaling in C3H/HeJ and C57BL/10ScCr mice: mutations in Tlr4 gene. Science 1998;282:2085–8.
[34] Nomura F, Akashi S, Sakao Y, Sato S, Kawai T, Matsumoto M, et al. Cutting edge: endotoxin tolerance in mouse peritoneal macrophages correlates with down-regulation of surface toll-like receptor 4 expression. Journal of Immunology 2000;164:3476–9.
[35] Boltana S, Roher N, Goetz FW, Mackenzie SA. PAMPs, PRRs and the genomics of gram negative bacterial recognition in fish. Developmental and Comparative Immunology 2011;35:1195–203.
[36] Xi Z, Ramirez JL, Dimopoulos G. The Aedes aegypti toll pathway controls dengue virus infection. PLoS Pathogens 2008;4:e1000098.
[37] Wang PH, Liang JP, Gu ZH, Wan DH, Weng SP, Yu XQ, et al. Molecular cloning, characterization and expression analysis of two novel Tolls (LvToll2 and LvToll3) and three putative Spatzle-like Toll ligands (LvSpz1-3) from Litopenaeus vannamei. Developmental and Comparative Immunology 2012;36:359–71.
[38] Wootton JC, Federhen S. Analysis of compositionally biased regions in sequence databases. Methods in Enzymology 1996;266:554–71.